Green Synthesized Zinc Oxide Nanoparticles Mediated by *Dysphania botrys* Extract: Structural Characterization and Biological Applications

Abdul Nasir [a†] Muhammad Tayyab [a †] Syed Jehangir Shah,[a] Muhammad Sayyar Khan [a] Heba I. Mohamed [b,*] Haiam O. Elkatry [c] Marwa Ezz El-Din Ibrahim [c] Hossam S. El-Beltagi [d] Mohamed El Oirdi [e] and Abdelrahman R. Ahmed [c,*]

* *Corresponding authors: Hebaibrahim79@gmail.com; arahmed@kfu.edu.sa*

DOI: 10.15376/biores.21.2.5106-5121

GRAPHICAL ABSTRACT

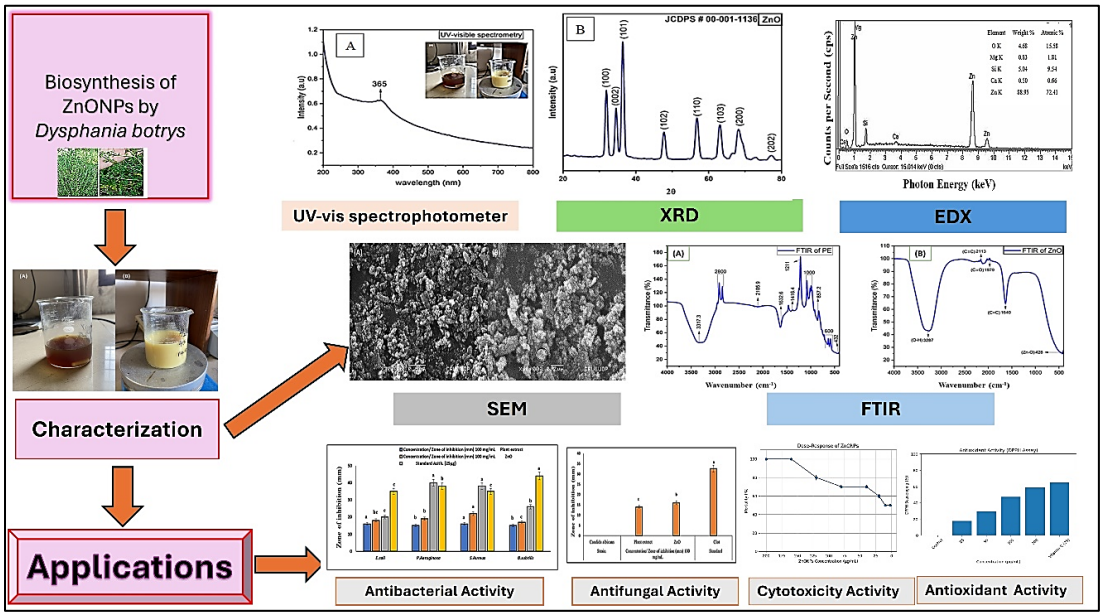

Green Synthesized Zinc Oxide Nanoparticles Mediated by *Dysphania botrys* Extract: Structural Characterization and Biological Applications

Abdul Nasir [a†] Muhammad Tayyab [a †] Syed Jehangir Shah,[a] Muhammad Sayyar Khan [a] Heba I. Mohamed [b,*] Haiam O. Elkatry [c] Marwa Ezz El-Din Ibrahim [c] Hossam S. El-Beltagi [d] Mohamed El Oirdi [e] and Abdelrahman R. Ahmed [c,*]

Zinc oxide nanoparticles (ZnONPs) were prepared using *Dysphania botrys* extract. Successful NPs formation was confirmed by UV-Vis spectroscopy with a characteristic absorbance peak at 365 nm. XRD analysis revealed a hexagonal wurtzite structure with an average crystallite size of 9.96 nm, while FTIR spectra indicated the involvement of plant phytochemicals in nanoparticle stabilization. SEM images showed predominantly hexagonal morphology, and EDX analysis confirmed high purity, with zinc and oxygen as the major elements. GC–MS profiling of the plant extract identified 26 bioactive compounds, with humulane-1,6-dien-3-ol (29.4%) as the most abundant. The biosynthesized ZnONPs exhibited pronounced antibacterial activity against both Gram-positive (*Staphylococcus aureus, Bacillus subtilis*) and Gram-negative (*Escherichia coli, Pseudomonas aeruginosa*) bacteria. Brine shrimp assays revealed concentration-dependent toxicity (100% mortality at ≥160 µg/mL), indicating that the biosynthesized ZnONPs had notable general cytotoxic potential, which warrants careful evaluation of environmental and biomedical safety. Meanwhile, DPPH assays revealed concentration-dependent antioxidant activity (58.8% at 200 µg/mL). Green synthesis using plant extracts has been proposed as a more environmentally benign approach and can reduce the use of hazardous reagents, although the resulting nanoparticles may still exhibit toxicity depending on their dose and properties.

DOI: 10.15376/biores.21.2.5106-5121

Keywords: Antioxidant activity; Antimicrobial activity; Characterization; Cytotoxic assay; Gas chromatography–mass spectrometry

Contact information: a: Institute of Biotechnology and Genetic Engineering, The University of Agriculture Peshawar, 25130 Peshawar, Pakistan; b: Department of Biological and Geological Sciences, Faculty of Education, Ain Shams University, Cairo, Egypt; c: Food and Nutrition Science Department, Agricultural Science and Food, King Faisal University, Al Ahsa 31982, Saudi Arabia; d: Agricultural Biotechnology Department, College of Agricultural and Food Science, King Faisal University, Al-Ahsa, 31982, Saudi Arabia; e: Department of Life Sciences, College of Science, King Faisal University, Al-Ahsa, 31982, Saudi Arabia; Corresponding authors: Hebaibrahim79@gmail.com; arahmed@kfu.edu.sa
†These authors contributed equally to this work.

INTRODUCTION

Green synthesis of zinc oxide nanoparticles (ZnONPs) using plant extracts has emerged as an eco-friendly alternative to conventional physical and chemical routes, which often involve high energy inputs and/or toxic precursors and solvents, which may raise

ecological and occupational safety concerns compared with plant-mediated approaches (Al-Rajhi *et al.* 2022; Abdelghany *et al.* 2023; Al-darwesh *et al.* 2024). Usually, nanoparticle size is between 1 nm and 100 nm, exhibiting distinctive features such as a large surface area-to-volume ratio and quantum effects, which contribute to their enhanced reactivity and multifunctionality (Ahmed *et al*. 2025).

ZnONPs are typically synthesized *via* chemical vapor deposition, sol-gel methods, hydrothermal methods, or co-precipitation methods. Although such approaches can produce excellent nanoparticles, they often involve the use of toxic chemicals and extreme conditions, which can have ecological potential risks (Jha *et al*. 2025). Green synthesis processes, prepared by bottom-up approaches and considered environmentally friendly, have sparked renewed interest in nanoparticle manufacturing in recent decades. This approach produces nanoparticles with a host of natural resources, such as bacteria and plants (Rashid *et al.* 2024). ZnONPs are commonly synthesized using plants or their parts, such as bark, stem, leaves, fruit, and seeds (Abdelhady *et al.* 2024; Alam *et al*. 2025). In these methods, plant phytochemicals such as alkaloids, flavonoids, terpenoids, polyphenols, and amino acids act as both reducing and capping agents, facilitating nanoparticle formation without the need for harmful intermediates (Jha *et al*. 2025). In biosynthesis, enzymes not only function as capping agents but also reduce electrons to produce a large number of nanoparticles with a very small size (Hayat *et al*. 2025).

ZnONPs have potent antimicrobial, antioxidant, and anti-inflammatory properties, making them ideal candidates for a wide range of biomedical applications such as drug delivery systems, wound healing, and therapeutic interventions (Ihsan *et al*. 2023). The capacity of zinc oxide (ZnO) to inhibit a wide range of harmful microorganisms, including fungi and both Gram-positive and Gram-negative bacteria, has made it recognized as a powerful antibacterial agent. Because of its small size, large surface area, and distinct surface reactivity, ZnO exhibits enhanced activity when it is in the form of nanoparticles (Hayat *et al*. 2025). The antibacterial activity of ZnONPs is mainly attributed to the generation of reactive oxygen species (ROS), which induce oxidative stress and cause severe damage to microbial cell membranes, proteins, and nucleic acids (Hayat *et al*. 2025). Further contributing to microbial cell death is the disruption of cellular metabolism and the compromising of membrane integrity caused by the release of Zn^{2+} ions (Sundrarajan *et al*. 2015).

Dysphania botrys is an annual herbaceous plant of the Amaranthaceae family. In folk medicine, *D. botrys* has been used to cure various diseases, including asthma, colds, influenza, headaches, liver and digestive disorders, and wound healing. It is also being investigated as a possible cancer treatment. *D. botrys* was chosen as a suitable plant for the preparation of ZnO nanoparticles through green synthesis due to their phytochemical characteristics and biological activities. This plant has a wide range of bioactive constituents that include flavonoids, phenolic acids, terpenoids, and essential oils (Dagni *et al.* 2022). These phytochemicals play an important role in both the reduction and stabilization of ZnO nanoparticles since they assist in transforming the metal precursors into ZnO nanoparticles while preventing the occurrence of agglomeration. Furthermore, due to the potent antioxidant capacity of *D. botrys*, the efficiency of the reaction is increased. Its antimicrobial properties could also contribute synergistically to the performance of the ZnO nanoparticles. The use of brine shrimp (*Artemia salina*) in a lethality bioassay is convenient because it is cost-effective and reliable, and results are available in a short time (Gangwar *et al*. 2024).

It is hypothesized here that *D. botrys* extract can mediate the green synthesis of ZnONPs and that these particles will show enhanced antimicrobial and antioxidant activities compared with the crude extract. This research paper highlights an environmentally friendly approach to producing zinc oxide nanoparticles using plant *D. botrys* for synthesis and stabilization. To our knowledge, there are no previous reports specifically describing *D. botrys*-mediated synthesis of ZnONPs; therefore, this work explores this plant as a new candidate for green ZnONPs production.

EXPERIMENTAL

Experimental Site

This study was conducted at the Institute of Biotechnology and Genetic Engineering, the University of Agriculture Peshawar, and PCSIR Laboratories.

Preparation of Extract

Fresh *D. botrys* plants were collected from the Medicinal Botanic Centre (PCSIR, Peshawar), washed with tap/distilled water, and shade-dried. The dried material was ground into a fine powder, and 15 g was mixed with 250 mL distilled water, heated at 100 °C for 1 h, and filtered (Whatman No. 1, 11 μm).

Preparation of Zinc Oxide Nanoparticles

The filtrate (pH 7.05) was combined with 0.1 M zinc acetate solution (2.195 g/100 mL), adjusted to pH 10 using NaOH, and stirred until the color changed from brown to yellow, indicating nanoparticle formation. The solution was centrifuged at 8,000 rpm for 25 min at 37 °C, washed thrice with distilled water, and the pellet was oven-dried at 65 °C for 24 h and ground into powder. Finally, the product was calcined at 400 °C for 1 h to obtain white ZnONPs, enhancing crystallinity and stability.

Physical Characterization of Zinc Oxide Nanoparticles

Characterization of ZnO nanoparticles (ZnONPs) was done using UV-Visible spectroscopy, X-ray diffraction (XRD), Fourier transform infrared spectroscopy (FTIR), and scanning electron microscopy (SEM). Absorbance measurements of ZnONPs solutions were taken by Cary 60 spectrophotometer (Agilent Technologies, Version 2.00, USA) for wavelengths ranging from 200 to 800 nm. For measurement, 1 mL of ZnONPs solution was prepared by dilution with distilled water using a quartz cuvette with a 1 cm path length and distilled water as the blank. XRD analysis was done using the Model 700 HS X-ray diffraction system (Shimadzu, Tokyo, Japan), which uses Cu Kα radiation with a wavelength of 1.5406 Å. The dried powder of zinc oxide nanoparticles was ground with an agate mortar and pestle and mounted on a glass holder. XRD pattern was obtained within the range of 10° to 80° 2θ angles.

FTIR spectra were obtained from plant extract as well as ZnONPs using a Bruker IR Biotyper device (Bruker Daltonics, Bremen, Germany). The ZnONPs and the freeze-dried plant extract powders were separately crushed with spectroscopic-grade potassium bromide (KBr) in the pellet form with the help of a hydraulic pellet press. FTIR spectra were taken between 4000 and 400 cm^{-1}. The SEM analysis of ZnONPs was performed using Hitachi TM1000 (52E-0101, Japan). A very little amount of dried ZnONPs was adhered on the carbon-coated aluminum stub by conductive double-sided carbon tape. The

specimen was sputter-free (or gold-coated) and analyzed under high vacuum to investigate surface morphology and size of particles.

Phytochemical Analysis of the Plant Extracts *via* Gas Chromatography-Mass Spectrometry

GC-MS analysis was conducted on a methanol extract to characterize the major volatile and semi-volatile phytochemicals of *D. botrys*. For plant extract preparation, 10 mL of methanol was added to the dried powder of *D. botrys* and kept at room temperature for 24 h to complete the extraction. The mixture was then filtered through a 0.45 µm membrane to remove residues, and the filtrate was concentrated using a rotary evaporator to obtain a solvent-free extract for GC-MS analysis. Phytochemical characterization was performed using a Shimadzu QP2010 Plus GC-MS system (Japan) following established protocols (Dagni *et al*. 2022). Operational parameters included a column oven temperature of 50 °C, an injection temperature of 250 °C, and spitless mode with a 1 µL injection volume. Separation was achieved using a 30 m × 0.25 µm capillary column, and 1 µL of the extract was analyzed for qualitative and quantitative identification of bioactive compounds.

Antimicrobial Activity

The antimicrobial activity of biosynthesized ZnONPs was assessed using the well diffusion method against five microorganisms: *Escherichia coli* ATCC 38738, *Pseudomonas aeruginosa* ATCC 39721, *Staphylococcus aureus* ATCC 36538, *Bacillus subtilis,* and *Candida albicans*. ZnONPs and *D. botrys* extract were prepared in dimethyl sulfoxide (DMSO) at a concentration of 100 mg/mL. After inoculating nutrient agar plates with microbial suspensions of 1×10^6 CFU/mL, wells were created, and each well received 100 µL of either the ZnONPs suspension, *D. botrys* extract, or DMSO (negative control). The plates were incubated at 37 °C for 24 h, and the zones of inhibition were measured using a Vernier caliper. This study demonstrated the potential of ZnONPs and *D. botrys* extract as antimicrobial agents (Dagni *et al*. 2022).

Antioxidant Activity

The antioxidant activity of ZnONPs was evaluated using the DPPH (2,2-diphenyl-1-picrylhydrazyl) radical scavenging assay (Alabri *et al*. 2014; Alawlaqi *et al.* 2023). A 0.1 mM DPPH solution was prepared by dissolving 3.94 mg of DPPH in 100 mL of DMSO and stored at 4 °C in the dark. For the assay, 1 mL of ZnONPs solutions (25, 50, 100, and 200 µg/mL in DMSO) was mixed with 1 mL of the DPPH solution, vortexed, and incubated in the dark at room temperature for 1.5 hours. Absorbance was then measured at 517 nm using a UV-visible spectrophotometer, with a blank sample and vitamin C (25 µg/mL of ascorbic acid) as a positive control. The percentage inhibition of DPPH radicals was calculated using the equation

$$\text{Percentage of inhibition (\%)} = (A_{\text{control}} - A_{\text{sample}})/(A_{\text{control}}) \times 100 \quad (1)$$

where A_{control} denotes the absorbance of the DPPH solution (without nanoparticles), and A_{sample} is the absorbance of the test sample (DPPH solution with nanoparticles).

Cytotoxic Activity

The cytotoxic potential of biosynthesized ZnONPs was evaluated using a brine shrimp lethality assay, based on the protocol by Younas *et al*. (2025). Artificial seawater

was prepared by dissolving 38 g of synthetic sea salt in one liter of distilled water, filtering it through Whatman filter paper, and autoclaving it at 121 °C and 15 psi for 20 minutes. Approximately 1 g of *Artemia salina* cysts was hatched in the sterilized artificial seawater under constant illumination at 37 °C for 24 h to produce swimming nauplii. The cytotoxicity of the ZnONPs was assessed using serial dilutions of ZnONPs suspensions at concentrations of 200, 160, 120, 80, 40, 20, 10, and 2 µg/mL. In each test, a prepared ZnONPs suspension was added to vials containing two milliliters of artificial seawater and ten nauplii, bringing the total volume to five milliliters. After 24 h of incubation at 37 °C, the nauplii were checked for mortality, and the percentage of lethality was calculated according to Eq. 2.

$$\text{Mortality (\%)} = (\text{CN} - \text{ST}) / \text{CN} \times 100 \quad (2)$$

where CN is the number of individuals in the control (or initial number), and ST denotes the number of surviving individuals after treatment.

Statistical Analysis

All experiments were performed in triplicate using three independent nanoparticle batches (biological replicates), and each measurement within an experiment was averaged from triplicate technical readings. The data were analyzed using SPSS statistical software (SAS Institute Inc., Cary, NC) with Duncan's multiple range tests following analysis of variance (ANOVA).

RESULTS AND DISCUSSION

After the initial steps of plant collection and leaf grinding, followed by the addition of zinc acetate dihydrate and crystal formations, the plants were first subjected to GC-MS analysis to find their bioactive compounds or metabolites, which gave the plants their therapeutic potential.

GC-MS Analysis of Plant Extract

GC–MS analysis of the methanolic extract was conducted to identify major phytochemicals; however, as it differs from the aqueous extract used for nanoparticle synthesis, the detected compounds should be considered putative contributors to the synthesis process. The GC-MS analysis of the *D. botrys* extract revealed the presence of 26 bioactive compounds, with several compounds exhibiting notably high concentrations, which were significant for the study as shown in Table 1. Humulane-1,6-dien-3-ol was the most abundant compound, constituting 29.4% of the total concentration, followed by guaiol at 16.0% and spathulenol at 12.2%. Hinesol also showed a substantial presence at 10.6%, while 1,2,3,6-tetramethylbicyclo[2.2.2]octa-2,5-diene contributed 7.60%. Other compounds with significant concentrations included juniper camphor (5.06%), tridecanoic acid (3.39%), elemol (2.62%), and isolongifolene, 4,5-dehydro- (2.45%). Some of the phytochemicals present in *D. botrys* may participate in the reduction and stabilization processes during ZnONP synthesis. In some plant-mediated systems, enzymes and phytochemicals can act as reducing and capping agents. In the case of *D. botrys*, the focus was on total phytochemical content rather than identifying specific enzymes.

Table 1. The Bioactive Compounds Identified in *D. botrys* Extracted through GC-MS Analysis

ID#	Name	Retention Time (min)	Area (%)	Conc. (%)
1	Undecane	9.563	201658	1.20
2	Dodecane	11.947	127982	0.76
3	Tridecane	14.266	56368	0.34
4	Hedycaryol	19.735	80271	0.48
5	Diepicedrene-1-oxide	20.924	18646	0.11
6	Longifolenaldehyde	21.454	26231	0.16
7	Andrographolide	21.567	122034	0.73
8	Tricyclo[3.2.1.02,7]oct-3-ene,2,3,4,5,-Tetramethyle	21.713	109521	0.65
9	Gamma. -Eudesmol	21.856	86356	0.51
10	Elemol	22.158	439972	2.62
11	(S)-*cis*-Verbenol	22.471	199048	1.18
12	Tetradecanoic acid	23.762	20945	0.12
13	Isolongifolene, 4,5-dehydro-	23.966	412031	2.45
14	Veridiflorol	23.768	28264	0.17
15	Guaiyl acetate	24.281	82791	0.49
16	Hinesol	24.770	1783650	10.61
17	Pentadecanal	25.010	70266	0.42
18	Spathulenol	25.628	2042921	12.16
19	Silana, dodecyldiethoxymethyl-	25.950	283684	1.69
20	1,2,3,6-Tetramethylbicyclo[2.2.2]octa-2,5-diene	26.039	1276506	7.60
21	Hexadecanoic acid, methyl ester	26.478	198055	1.18
22	Juniper camphor	26.947	850794	5.06
23	Tridecanoic acid	27.162	569679	3.39
24	Gauiol	27.299	2686777	15.99
25	Ent-spathulenol	28.516	104666	0.62
26	Humulane-1,6-dien-3-ol	29.042	4945108	29.43

These results are consistent with previous studies that found similar compounds in other plant species. For example, spathulenol was the predominant compound in *Psidium guineense* essential oil (80.7%) (do Nascimento *et al*. 2018). Hinesol was also one of the most abundant components (45.7%) in *Atractylodes lancea* (Ouyang *et al*. 2012), and 1,2,3,6-Tetramethylbicyclo[2.2.2]octa-2,5-diene was detected in *Atractylodes macro-cephala* and *Astragalus membranaceus* at 0.4% to 0.5% (Li *et al*. 2013). The oxygenated terpenoids detected using GC–MS (such as guaiol, spathulenol, hinesol, and elemol) that have hydroxyl groups function as reducing agents that reduce zinc ions (Zn^{2+}) to zinc oxide (ZnO), while at the same time functioning as capping agents. This process entails reducing zinc ions to zinc hydroxide ($Zn(OH)_2$).

Analysis Through UV-visible Spectrometry

Dysphania botrys plant extracts were used to synthesize ZnONPs, with the initial verification confirmed by observing color changes and pH shifts upon the addition of zinc acetate dihydrate (Fig. 1A). The UV spectroscopy confirmed the formation of ZnONPs.

The UV spectrum of ZnONPs synthesized from *D. botrys* extract is shown in Fig. 1A. The highest peak observed in the sample was at 365 nm, with an absorbance of 0.62, which demonstrates the presence of ZnONPs. The optimal absorption spectrum for ZnONPs typically lies within the range of 200 to 800 nm. The optical and structural properties of the biosynthesized ZnONPs exhibit significant variation depending on the type of plant material used, the types of ZnO precursors, and the protocol used. This aligns with previous reports: 375 nm for *Plectranthus amboinicus* (Vijayakumar *et al*. 2015), 375 nm for *Aloe vera* (Ali *et al*. 2016), and 365 nm for *Salvadora persica* (Al Rahbi *et al*. 2024).

X-Ray Diffraction for Crystalline Structure Analysis of ZnONPs

As depicted in Fig. 1B, the XRD pattern exhibited distinct diffraction peaks corresponding to the hexagonal wurtzite structure of ZnO, which aligned well with the standard reference (JCPDS card No. 00-001-1136). The prominent diffraction peaks were observed at 2θ values of 31.7°, 34.4°, 36.2°, 47.5°, 56.6°, 62.9°, 68.4°, and 77.1°, which are indexed to the (100), (002), (101), (102), (110), (103), (200), and (202) crystallographic planes, respectively. The sharpness and high intensity of the diffraction peaks indicate the excellent crystallinity of the synthesized ZnONPs. Furthermore, the absence of any additional peaks in the XRD pattern confirms the phase purity of the material, with no detectable secondary phases or impurities. The average crystallite size of the nanoparticles, calculated using the Debye-Scherrer formula, was 9.96 nm. These results collectively demonstrate the successful synthesis of highly crystalline and phase-pure ZnONPs. Similar findings have been reported for ZnONPs synthesized using *Agathosma betulina* extract (Thema *et al*. 2015) and *Carica papaya* leaf extract (Rathnasamy *et al*. 2017). According to the Debye–Scherrer equation, the average crystallite size of the prepared ZnONPs was calculated to be 9.96 nm. These findings are consistent with previously reported crystallite sizes of 17.47, 13.51, 10.34, and 9.04 nm for ZnONPs prepared from *Camellia sinensis* leaf extract at variable concentrations (Nava *et al*. 2017).

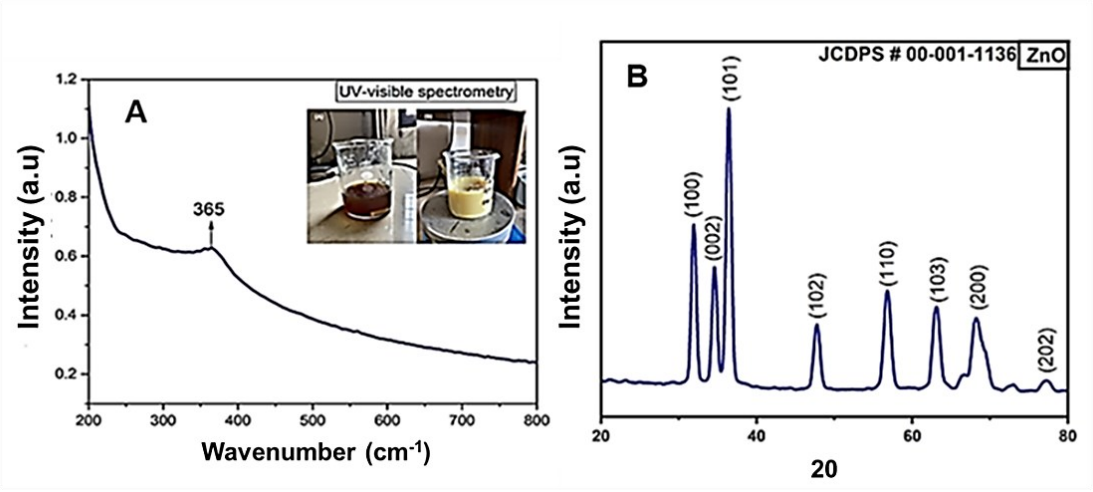

Fig. 1. UV-visible spectral analyses of biosynthesized ZnONPs showing the highest peak at 365 nm (A); and XRD graph showing Bragg reflection indicating the presence of biosynthesized ZnONPs (B)

Fourier Transform Infrared Spectroscopy

The FTIR analysis of both the plant extract and synthesized ZnONPs revealed a crucial interconnection, highlighting the dual role of phytochemicals in green synthesis as shown in Fig. 2. The presence of hydroxyl (O–H) and carbonyl (C=O) groups in both samples (at 3317 cm^{-1} and 1632 cm^{-1} in the extract, at 3287 cm^{-1} and 1640 cm^{-1} in ZnONPs) suggests that these functional groups act as reducing agents during nanoparticle formation and act as stabilizing agents through surface interactions. The shift in the O–H peak from 3317 cm^{-1} to 3287 cm^{-1} indicates partial consumption of hydroxyl groups during reduction, while the persistence of C=O peaks imply stabilization *via* chelation. The distinct Zn–O peak at 428 cm^{-1} in ZnO spectra confirms successful nanoparticle synthesis. Overall, this analysis supports the role of plant-derived compounds in both reducing metal ions and stabilizing the resulting nanoparticles, aligning with green chemistry principles. Similar to the results observed for other green-synthesized ZnONPs, *e.g.*, Zn–O peaks at 435 cm^{-1} in *Cayratia pedata* biomass-mediated synthesis (Jayachandran *et al*. 2021) and 625.1 cm^{-1} for *Citrus* medica-derived NPs (Sowmya *et al*. 2024).

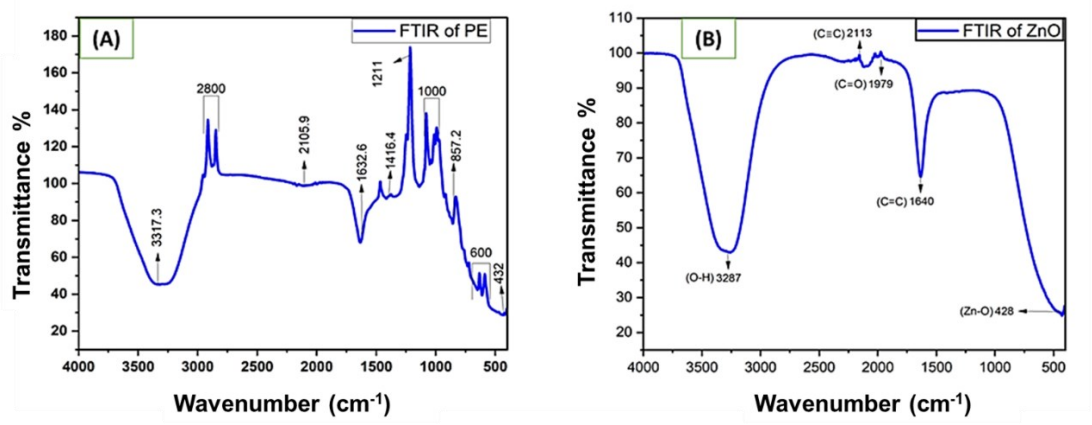

Fig. 2. FTIR spectra showing the plant extract (A) and the biosynthesized ZnONPs (B)

Scanning Electron Microscope

The morphological characteristics of the green synthesized ZnONPs were analyzed using SEM, as shown in Fig. 3.

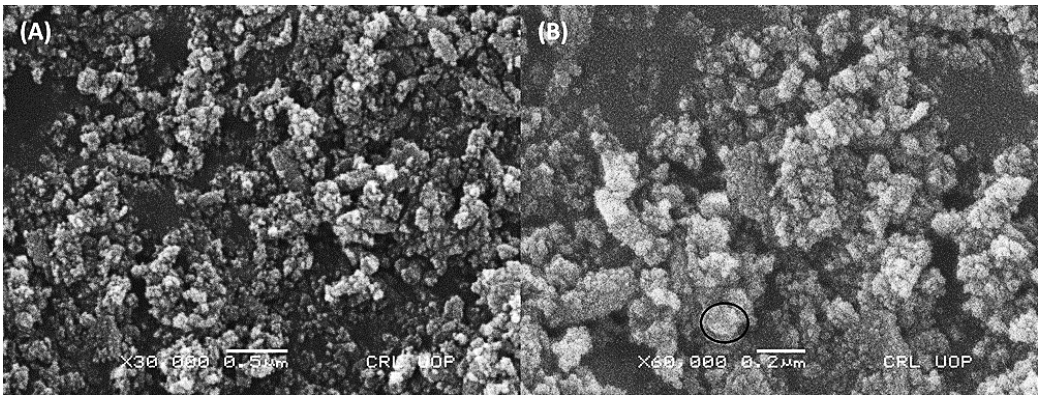

Fig. 3. Scanning electron microscopy (SEM) images of biosynthesized ZnO nanoparticles (ZnONPs) at different magnifications: (A) 0.5 µm scale bar and (B) 0.2 µm scale bar, showing the morphology and size distribution of the nanoparticles.

Based on the SEM analysis, the nanoparticles exhibited predominantly hexagonal particles, showcasing a highly uniform and consistent morphology. The distinct hexagonal structure of the ZnONPs highlights their crystalline nature and suggests a high degree of purity and precision in the synthesis process. These results agree with prior findings, where the ZnONPs synthesized from grains of *Echinochloa frumentacea* (Velsankar *et al*. 2020) displayed primarily a hexagonal morphology.

Energy Dispersive Spectroscopy of ZnONPs

The spectrum revealed the presence of primary elements, specifically zinc (Zn) and oxygen (O), which confirms the successful biosynthesis of ZnONPs. EDX spectra showed zinc and oxygen as the major elements, along with minor amounts of Mg, Si, and Ca, consistent with ZnO nanoparticles bearing trace inorganic impurities, as illustrated in Fig. 4. Previous studies have reported similar findings for the synthesis of ZnO from *Myristica fragrans* (Faisal *et al*. 2021) and from *Ipomoea pescaprae* (Venkateasan *et al*. 2017).

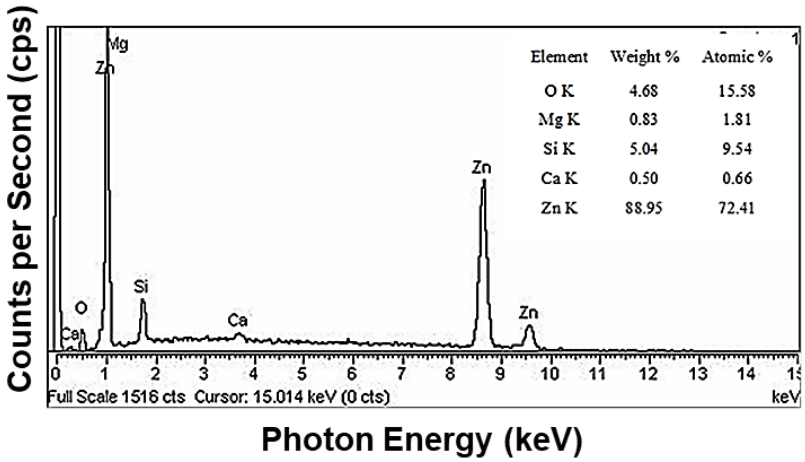

Fig. 4. EDX spectrum of green synthesized ZnONPs, which indicates different elements

Antibacterial Assay

The antibacterial activity of biosynthesized ZnONPs using *D. botrys* extract showed superior efficacy against both Gram-negative (*E. coli*, *P. aeruginosa*) and Gram-positive (*S. aureus*, *B. subtilis*) bacteria compared to the plant extract alone (Fig. 5). The plant extract (positive control) showed inhibition zones of 16±0.3 mm (*E. coli*), 15±0.1 mm (*P. aeruginosa*), 16±0.2 mm (*S. aureus*), and 14±0.1 mm (*B. subtilis*), while DMSO (negative control) had no inhibition. ZnONPs demonstrated significantly enhanced antibacterial activity, with inhibition zones of 18±0.2 mm (*E. coli*), 19±0.3 mm (*P. aeruginosa*), 22±0.3 mm (*S. aureus*), and 17±0.2 mm (*B. subtilis*), as shown in Fig. 5. When compared to standard antibiotics, ZnONPs exhibited competitive antimicrobial potential, particularly against *S. aureus*, where their inhibition zone (22±0.4 mm) was relatively close to that of ciprofloxacin (26±0.4 mm). These results highlight the promising role of *D. botrys*-mediated ZnONPs as eco-friendly antimicrobial agents. Their potency per unit mass was lower than that of standard antibiotics, and further optimization is needed. Similar results were reported for Myristica fragrans-derived ZnONPs against *E. coli*, *P. aeruginosa*, *S. aureus*, and *B. subtilis* (Faisal *et al*. 2021; Qanash *et al.* 2024) and ZnO from *Ailanthus altissima* fruit extracts (Awwad *et al*. 2020; Selim *et al.* 2025).

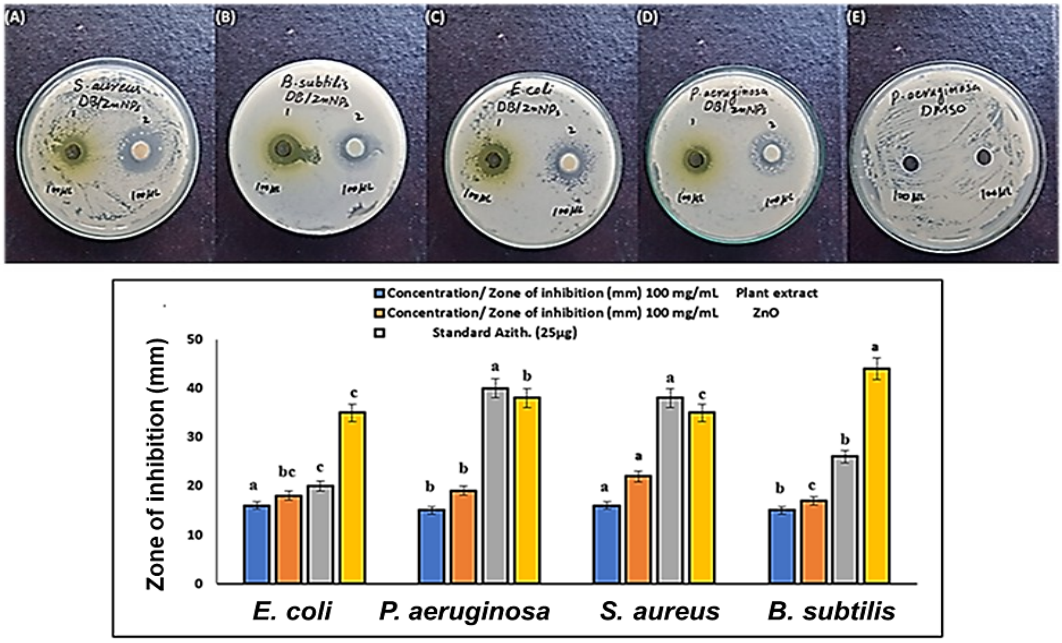

Fig. 5. Antibacterial activity against plant extract/ZnONPs: (A) *S. aureus*, (B) *B. subtilis*, (C) *E. coli*, (D) *P. aeruginosa*, (E) DMSO as a negative control, and the zone of inhibition of concentrations of ZnO (100 mg/mL), plant extract, and standard antibiotics (azithromycin and ciprofloxacin). The data represents the meaning of three replicates, with ±SE. Mean values in each bar followed by different lowercase letters are significantly different according to Duncan's multiple range test at $P < 0.05$.

Antifungal Assay

Green-synthesized ZnONPs demonstrated promising antifungal activity against *C. albicans*, with an inhibition zone of 16±0.2 mm, surpassing the plant extract's 14±0.1 mm, as shown in Fig. 6.

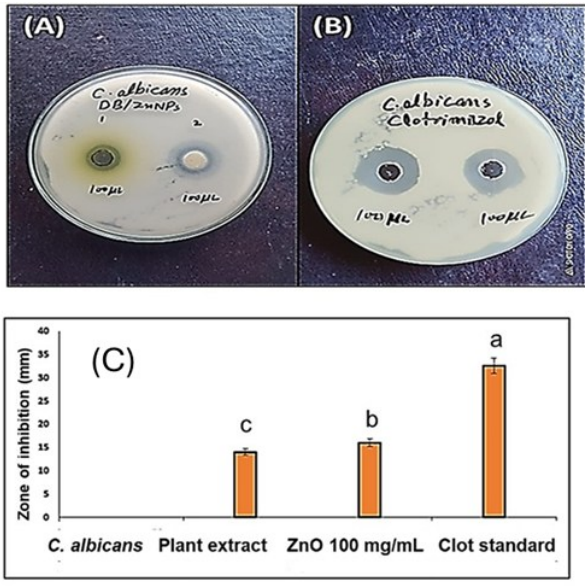

Fig. 6. Antifungal activity of plant extract (A), ZnONPs against *C. albicans* (B) and (C) zone inhibition (mm). Positive control of clotrimazole against *C. albicans* in replicates. The data represents the mean of three replicates, with ±SE. Mean values in each bar followed by different lowercase letters are significantly different according to Duncan's multiple range test at $P < 0.05$.

This was less effective than clotrimazole (32.5±0.4 mm), which was used as a positive control. ZnONPs show potential as eco-friendly antifungal agents. Similar antifungal activity was also reported for ZnONPs synthesized from *Salvia officinalis* leaf extract against *C. albicans* (Yassin *et al*. 2023). The toxicity may involve oxidative stress and Zn^{2+} release, as reported elsewhere for ZnONPs, although we did not measure ROS or ion release in the present study.

Cytotoxic Assay

The cytotoxic potential of *D. botrys*-mediated ZnONPs was evaluated using a brine shrimp lethality assay over 24 h, revealing a strong concentration-dependent toxicity profile (Table 2). Notably, at 160 and 200 µg/mL, the ZnONPs induced 100% mortality within 24 h, signifying complete lethality. Lower concentrations also exhibited significant toxicity, with 80 and 40 µg/mL both causing 70% mortality, followed by 20 µg/mL (60%) and 10 µg/mL (50%). Remarkably, even at the lowest tested concentration (2 µg/mL), a persistent 50% mortality rate was observed after 24 h, highlighting the potent bioactivity of the synthesized nanoparticles. The IC50 value was notably low, indicating a strong cytotoxic effect, which is consistent with reports attributing ZnONP-induced oxidative stress and Zn^{2+} ion release as primary mechanisms of toxicity in *Artemia salina*. These findings highlight the potential of biologically synthesized ZnONPs as highly bioactive agents, warranting further exploration of their biomedical and environmental applications. Faisal *et al*. (2021) verify concentration-dependent toxicity on synthesized ZnONPs, possibly involving oxidative stress and bioaccumulation mechanisms. These findings highlight their dual potential in biomedical and environmental applications, despite their ecotoxicological risks.

Table 2. Cytotoxicity of ZnONPs on Brine Shrimp

ZnONPs Concentration (µg/mL)	200	160	120	80	40	20	10	2
Mortality (%)	100±0.0	100±0.0	80±3.0	70±2.0	70±2.0	60±2.0	50±1.0	50±1.0

The data represents the meaning of three replicates, with ±SE.

Antioxidant Assay

The antioxidant potential of the green-synthesized ZnONPs was assessed using the DPPH (2,2-diphenyl-1-picrylhydrazyl) radical scavenging assay (Table 3). The results revealed a concentration-dependent increase in antioxidant activity, demonstrating the nanoparticles' ability to scavenge free radicals effectively. At 25, 50, 100, and 200 µg/mL concentrations, the nanoparticles exhibited DPPH scavenging activities of 17.6%, 29.4%, 47.1%, and 58.8%, respectively. The corresponding absorbance values at 517 nm decreased progressively from 0.70 to 0.35, indicating a rise in radical scavenging efficiency with increasing nanoparticle concentration. Ascorbic acid (25 µg/mL), used as a standard antioxidant, showed 64.7% DPPH scavenging activity with an absorbance of 0.30, serving as a reference for comparison, as shown in Table 3. The results demonstrate the significant antioxidant potential of the biosynthesized ZnONPs, with their efficacy enhancing notably at higher concentrations. This suggests their promising role as an antioxidant agent in various applications. These results are in agreement with the previous reports of ZnONPs

derived from sea lavender, which were dose-dependent (75.2% at 1000 µg/mL) (Naiel *et al*. 2022).

Table 3. DPPH Radical Scavenging Activity of ZnONPs

Concentration (µg/mL)	Absorbance at 517 nm	% DPPH Scavenging
Control	0.85±0.01	
25	0.70±0.01	17.6 %
50	0.60±0.01	29.4%
100	0.45±0.01	47.1%
200	0.35±0.01	58.8%
Vitamin C (25 µg/mL)	0.30±0.01	64.7%

The data represents the mean of three replicates, with ±SE.

CONCLUSIONS

1. Many of the identified compounds, *e.g.*, humulane-1,6-dien-3-ol (29.4%) and gauiol (16.0%), using GC-MS analysis, have been reported in the literature to possess antimicrobial, antioxidant, or anti-inflammatory activities, suggesting that *D. botrys* contains bioactive constituents that could contribute to the observed properties.
2. EDX elemental analysis confirmed high-purity ZnONPs composed mainly of zinc (72%) and oxygen (15%), with "ZnO-rich" nanoparticles with zinc and oxygen as predominant elements, accompanied by small amounts of other elements.
3. The biosynthesized ZnONPs exhibited strong antimicrobial activity, producing inhibition zones ranging from 16 to 22 mm against *E. coli, P. aeruginosa, S. aureus, B. subtilis*, and *C. albicans*.
4. Cytotoxicity assays demonstrated high toxicity toward brine shrimp larvae, indicating notable cytotoxic potential.
5. Antioxidant activity, assessed by the DPPH assay, showed a 58.5% free-radical scavenging efficiency, reflecting substantial antioxidant capacity.
6. Specifically, the findings provide partial support for the hypothesis formulated, because the biosynthesized ZnONPs showed a markedly higher antimicrobial and antioxidant activity than that of the crude extract, but the degree of increase differed for various microorganisms.
7. The *D. botrys*-mediated ZnONPs displayed *in vitro* antibacterial and antifungal activity and showed measurable antioxidant activity, along with notable toxicity in the brine shrimp assay. These preliminary findings indicate that *D. botrys* extract can serve as a green route to synthesize ZnONPs, but further work is required to optimize nanoparticle properties, fully elucidate mechanisms, and rigorously evaluate safety in mammalian and environmental models before any biomedical or environmental applications can be considered.

FUNDING

Supported by the Deanship of Scientific Research, Vice Presidency for Graduate Studies, and Scientific Research at King Faisal University, Saudi Arabia (Grant No. KFU260117).

ACKNOWLEDGMENTS

We thank the Deanship of Scientific Research, Vice Presidency for Graduate Studies and Scientific Research, King Faisal University, Saudi Arabia (Grant No. KFU260117), for supporting this research work.

Conflict of Interest

The authors declare no competing interests.

REFERENCE CITED

Abdelghany, T. M., Al-Rajhi, A. M. H., Yahya, R., Bakri, M. M., Al Abboud, M. A., Yahya, R., Qanash, H., Bazaid, A. S., and Salem, S. S. (2023). "Phytofabrication of zinc oxide nanoparticles with advanced characterization and its antioxidant, anticancer, and antimicrobial activity against pathogenic microorganisms," *Biomass Conv. Bioref.* 13, 417-430. https://doi.org/10.1007/s13399-022-03412-1

Abdelhady, M. A., Abdelghany, T. M., Mohamed, S. H., and Abdelbary, S. A. (2024). "Impact of green synthesized zinc oxide nanoparticles for treating dry rot in potato tubers," *BioResources* 19(2), 2106-2119. https://doi.org/10.15376/biores.19.2.2106-2119

Alam, K., Din, I. U., Tariq, S., Hayat, K., Khan, F. U., Khan, M., and Mohamed, H. I. (2025). "Green synthesis and characterization of zinc oxide nanoparticles biosynthesized from *Butea monosperma* flowers and *Glycyrrhiza glabra* roots and their antioxidant and antibacterial properties," *Appl Biochem Biotechnol*. 197(3), 1630-1649. https://doi.org/10.1007/s12010-024-05102-2

Alawlaqi, M. M., Al-Rajhi, A. M. H., Abdelghany, T. M., Ganash, M., and Moawad, H. (2023). "Evaluation of biomedical applications for linseed extract: Antimicrobial, antioxidant, anti-diabetic, and anti-inflammatory activities *in vitro*," *J. Funct. Biomater.* 14, article 300. https://doi.org/10.3390/jfb14060300

Al-Rajhi, A. M., Yahya, R., Bakri, M. M., Yahya, R., and Abdelghany, T. M. (2022). "*In situ* green synthesis of Cu-doped ZnO based polymers nanocomposite with studying antimicrobial, antioxidant and anti-inflammatory activities," *Appl Biol Chem.* 65, article 35. https://doi.org/10.1186/s13765-022-00702-0

Ahmed, A. R., and Mohamed, H. I. (2025). "Nanofertilizers: Smart solutions for sustainable agriculture and the global water crisis," *Planta* 262(2), article 26. https://doi.org/10.1007/s00425-025-04737-7

Al Rahbi, A. S., Al Mawali, A. H., Al Rawahi, S. S., Al Dighishi, R. K., Al Abri, F. A., Ahmed, A., and Rahman, S. (2024). "Green synthesis of zinc oxide nanoparticles from Salvadora persica leaf extract: Characterization and studying methyl orange removal by adsorption," *Water Practice Technol.* 19(4), 1219-1231. https://doi.org/10.2166/wpt.2024.042

Alabri, T. H. A., Al Musalami, A. H. S., Hossain, M. A., Weli, A. M. and Al-Riyami, Q. (2014). "Comparative study of phytochemical screening, antioxidant and antimicrobial capacities of fresh and dry leaves crude plant extracts of *Datura metel* L," *J. King Saud Univ Sci.* 26(3), 237-243. https://doi.org/10.1016/j.jksus.2013.07.002

Al-darwesh, M. Y., Ibrahim, S. S. and Hamid, L. L. (2024). "*Ficus carica* latex mediated biosynthesis of zinc oxide nanoparticles and assessment of their antibacterial activity and biological safety," *Nano-Structures Nano-Objects* 38, article 101163. https://doi.org/10.1016/j.nanoso.2024.101163

Ali, K., Dwivedi, S., Azam, A., Saquib, Q., Al-Said, M. S., Alkhedhairy, A. A., and Musarrat, J. (2016). "*Aloe vera* extract functionalized zinc oxide nanoparticles as nanoantibiotics against multi-drug resistant clinical bacterial isolates," *J. Colloid Interface Sci.* 472, 145-156. https://doi.org/10.1016/j.jcis.2016.03.021

Awwad, A. M., Amer, M. W., Salem, N. M., and Abdeen, A. O. (2020). "Green synthesis of zinc oxide nanoparticles (ZnO-NPs) using *Ailanthus altissima* fruit extracts and antibacterial activity," *Chem Int.* 6(3), 151-159. https://doi.org/10.5281/zenodo.3559520

Dagni, A., Hegheș, S. C., Suharoschi, R., Pop, O. L., Fodor, A., Vulturar, R., Cozma, A., Aniq filali, O., Vodnar, D. C., Soukri, A., and El Khalfi, B. (2022). "Essential oils from *Dysphania* genus: Traditional uses, chemical composition, toxicology, and health benefits," *Front Pharmacol.* 13, article 1024274. https://doi.org/10.3389/fphar.2022.1024274

do Nascimento, K. F., Moreira, F. M. F., Santos, J. A., Kassuya, C. A. L., Croda, J. H. R., Cardoso, C. A. L., and Formagio, A. S. N. (2018). "Antioxidant, anti-inflammatory, antiproliferative and antimycobacterial activities of the essential oil of *Psidium guineense* Sw. and spathulenol," *J. Ethnopharmacol.* 210, 351-358. https://doi.org/10.1016/j.jep.2017.08.030

Faisal, S., Jan, H., Shah, S. A., Shah, S., Khan, A., Akbar, M. T., Rizwan, M., Jan, F., Wajidullah, Akhtar, N. and Khattak, A. (2021). "Green synthesis of zinc oxide (ZnO) nanoparticles using aqueous fruit extracts of *Myristica fragrans*: Their characterizations and biological and environmental applications," *ACS Omega* 6(14), 9709-9722. https://doi.org/0.1021/acsomega.1c00310

Gangwar, J., Balasubramanian, B., Pratap Singh, A., Meyyazhagan, A., Pappuswamy, M., Alanazi, A. M., Rengasamy, K. R., and Kadanthottu Sebastian, J. (2024). "Biosynthesis of zinc oxide nanoparticles mediated by *Strobilanthes hamiltoniana*: Characterizations and its biological applications," *Kuwait J. Sci.* 51(1), article 100102. https://doi.org/10.1016/j.kjs.2023.07.008

Hayat, K., Din, I. U., Alam, K., Khan, F. U., Khan, M., and Mohamed, H. I. (2025). "Green synthesis of zinc oxide nanoparticles using plant extracts of *Fumaria officinalis* and *Peganum harmala* and their antioxidant and antibacterial activities," *Biomass Conv Bioref.* 15(6), 9565-9579. https://doi.org/10.1007/s13399-024-05804-x

Ihsan, M., Din, I. U., Alam, K., Munir, I., Mohamed, H. I. and Khan, F. (2023). "Green fabrication, characterization of zinc oxide nanoparticles using plant extract of *Momordica charantia* and *Curcuma zedoaria* and their antibacterial and antioxidant activities," *App. Biochem and Biotechnol.* 195(6), 3546-3565. https://doi.org/10.1007/s12010-022-04309-5

Jayachandran, A., Aswathy, T. R., and Nair, A. S. (2021). "Green synthesis and characterization of zinc oxide nanoparticles using *Cayratia pedata* leaf extract," *Biochem. Biophy. Rep.* 26, article 100995. DOI: 0.1016/j.bbrep.2021.100995.

Jha, Y., Mohamed, H. I., Elkatry, H. O., and Ahmed, A. R. (2025). "Harnessing biologically synthesized nanomaterials for their antimicrobial potential in crop protection," *Physiol. Mol. Plant Pathol.* 139, article 102779. https://doi.org/10.1016/j.pmpp.2025.102779

Li, J., Li, F., Xu, Y., Yang, W., Qu, L., Xiang, Q., Liu, C., and Li, D. (2013). "Chemical composition and synergistic antioxidant activities of essential oils from *Atractylodes macrocephala* and *Astragalus membranaceus*," *Nat Prod Commun.* 8(9), 1321-1324.

Naiel, B., Fawzy, M., Halmy, M. W. A., and Mahmoud, A. E. D. (2022). "Green synthesis of zinc oxide nanoparticles using sea lavender (*Limonium pruinosum* L. Chaz.) extract: Characterization, evaluation of anti-skin cancer, antimicrobial and antioxidant potentials," *Sci. Rep.* 12(1), article 20370. https://doi.org/10.1038/s41598-022-24805-2

Nava, O. J., Luque, P. A., Gómez-Gutiérrez, C. M., Vilchis-Nestor, A. R., Castro-Beltrán, A., Mota-González, M. L., and Olivas, A. (2017). "Influence of *Camellia sinensis* extract on zinc oxide nanoparticle green synthesis," *J. Mol. Struct.* 1134, 121-125. https://doi.org/10.1016/j.molstruc.2016.12.069

Ouyang, Z., Zhang, L., Zhao, M., Wang, P., Wei, Y., and Fang, J. (2012). "Identification and quantification of sesquiterpenes and polyacetylenes in *Atractylodes lancea* from various geographical origins using GC-MS analysis," *Revista Brasileira de Farmacognosia* 22, 957-963. https://doi.org/10.1590/S0102-695X2012005000051

Qanash, H., Bazaid, A. S., Alharazi, T., Barnawi, H., Alotaibi, K., Shater, A. R. M. and Abdelghany, T. M. (2024). "Bioenvironmental applications of myco-created bioactive zinc oxide nanoparticle-doped selenium oxide nanoparticles," *Biomass Conv. Bioref.* 14, 17341-17352. https://doi.org/10.1007/s13399-023-03809-6

Rashid, M. U., Shah, S. J., Attacha, S., Khan, L., Saeed, J., Shah, S. T., and Mohamed, H. I. (2024). "Green synthesis and characterization of zinc oxide nanoparticles using *Citrus limetta* peels extract and their antibacterial activity against brown and soft rot pathogens and antioxidant potential," *Waste Biomass Valor.* 15(6), 3351-3366. https://doi.org/10.1007/s12649-023-02389-w

Rathnasamy, R., Thangasamy, P., Thangamuthu, R., Sampath, S., and Alagan, V. (2017). "Green synthesis of ZnO nanoparticles using *Carica papaya* leaf extracts for photocatalytic and photovoltaic applications," *J. Mater Sci.: Mater. Electron.* 28(14), 10374-10381. https://doi.org/10.1007/s10854-017-6807-8

Selim, S., Abdelghany, T. M., Almuhayawi, M. S., Nagshabandi, M. K., Tarabulsi, M. K., Elamir, M. Y., Alharbi, A. A., and Al Jaouni, S. K. (2025). "Biosynthesis and activity of Zn-MnO nanocomposite *in vitro* with molecular docking studies against multidrug resistance bacteria and inflammatory activators," *Sci. Rep.* 15(1), article 2032. https://doi.org/10.1038/s41598-024-85005-8

Sowmya, B., Saravanan, P., Rajeshkannan, R., Rajasimman, M., and Venkatkumar, S. (2024). "Facile verdant approach on zirconia-doped zinc oxide nanoparticles (Zr-ZnONPs) using *Citrus medica* fruit: antibacterial and anti-inflammatory activity," *Biomass Conv Bioref.* 14(20), 25985-25993. DOI: 10.1007/s13399-023-04652-5.

Sundrarajan, M., Ambika, S. and Bharathi, K. (2015). "Plant-extract mediated synthesis of ZnO nanoparticles using *Pongamia pinnata* and their activity against pathogenic bacteria," *Adv. Powder Technol.* 26(5), 1294-1299. DOI: 10.1016/j.apt.2015.07.001.

Thema, F. T., Manikandan, E., Dhlamini, M. S., and Maaza, M. J. M. L. (2015). "Green synthesis of ZnO nanoparticles *via Agathosma betulina* natural extract," *Mat Lett.* 161, 124-127. DOI: 10.1016/j.matlet.2015.08.052.

Velsankar, K., Sudhahar, S., Parvathy, G., and Kaliammal, R. (2020). "Effect of cytotoxicity and antibacterial activity of biosynthesis of ZnO hexagonal shaped nanoparticles by *Echinochloa frumentacea* grains extract as a reducing agent," *Mat. Chem. Physics*. 239, article 121976. DOI: 10.1016/j.matchemphys.2019.121976.

Venkateasan, A., Prabakaran, R., and Sujatha, V. (2017). "Phytoextract-mediated synthesis of zinc oxide nanoparticles using aqueous leaves extract of *Ipomoea pescaprae* (L). R. br revealing its biological properties and photocatalytic activity," *Nanotechnol Environ Eng.* 2, 8. https://doi.org/10.1007/s41204-017-0018-7

Vijayakumar, S., Vinoj, G., Malaikozhundan, B., Shanthi, S., and Vaseeharan, B. (2015). "*Plectranthus amboinicus* leaf extract mediated synthesis of zinc oxide nanoparticles and its control of methicillin resistant *Staphylococcus aureus* biofilm and blood sucking mosquito larvae," *Spectrochim. Acta A Mol. Biomol. Spectrosc.* 137, 886-891. https://doi.org/10.1016/j.saa.2014.08.064

Yassin, M. T., Al-Otibi, F. O., Al-Askar, A. A., and Elmaghrabi, M. M. (2023). "Synergistic anticandidal effectiveness of greenly synthesized zinc oxide nanoparticles with antifungal agents against nosocomial candidal pathogens," *Microorganisms* 11(8), article 1957. https://doi.org/10.3390/microorganisms11081957

Younas, S., Khan, S., Murad, W., Sama, N. U., Ullah, Z., Kamran, K., Haq, S. I. U., and Mohamed, H. I. (2025). "Synthesis of silver nanoparticles using a novel stem extract of *Anabasis lachnantha* and their insecticidal, antioxidant, and antimicrobial effects," *J. Microbiol. Biotechnol. Food Sci.* 14(6), e12686-e12686. https://doi.org/10.55251/jmbfs.12686

Article submitted: January 7, 2026; Peer review completed: April 4, 2026; Revised version received and accepted: April 15, 2026; Published: April 24, 2026.
DOI: 10.15376/biores.21.2.5106-5121